STRUCTURE CHARACTERISTICS OF A ^{4}He NUCLEUS WITHIN THE MICROSCOPIC APPROACH

B.E. GRINYUK[1], D.V. PIATNYTSKYI[2], I.V. SIMENOG[1,2]

[1]M.M. Bogolyubov Institute for Theoretical Physics, Nat. Acad. Sci. of Ukraine
(14b, Metrolohichna Str., Kyiv 03143, Ukraine; e-mail: bgrinyuk@bitp.kiev.ua),

[2]Taras Shevchenko Kyiv National University
(6, Academician Glushkov Prosp., Kyiv 03127, Ukraine)

UDC 539.172

A precise study of the energy, radii, and basic structure functions of a ^{4}He nucleus is carried out using the variational method with optimized Gaussian bases. We consider the Minnesota and AT potentials, as well as a new NN-potential K1 proposed to achieve a concordance of the main low-energy two-nucleon parameters and the energies of three- and four-nucleon nuclei. The analysis of the structure characteristics of a ^{4}He nucleus is carried out. To achieve the precise accuracy in calculations, we use the advantages of the representation without isospin.

1. Introduction

The precise studies of the few-nucleon systems in bound states are appreciably developing due to the use of powerful variational methods [1–3] which open a possibility to study the finest structural characteristics of the nuclear systems. The elaborated representation without isospin [4, 5] gives us additional essential advantages for studying the systems of few nucleons due to a significant reduction of the number of independent equations for the spatial components of wave functions, which essentially simplifies the calculational problem. The variational method with the use of a Gaussian basis has proved its high efficiency and accuracy [3] in the applications to a number of different few-particle problems, which is particularly true while using the special schemes for the optimization of Gaussian bases [6–8]. This approach enables us to achieve a high controllable precision in the calculations of the energy levels and the corresponding wave functions even for loosely bound near-threshold states [9].

In the present work, we study the properties of a four-nucleon nucleus ^{4}He using the variational method with some schemes of optimization of the Gaussian bases and using the representation without isospin (reducing the problem to the system of only two equations [4] for the spatial components of the wave function instead of twelve ones in the traditional isospin formalism). The binding energy and radii, as well as the main structure functions of this nucleus (density distributions, formfactors, pair correlation functions, and momentum distributions) are studied within the microscopic approach. We use the known popular interaction potentials, the Minnesota (further denoted by M) and Afnan–Tang (further AT) potentials, which give reasonable values for the binding energy and radius of a ^{4}He nucleus from the qualitative point of view. Intending, in the future, to construct the nuclear potentials for a satisfactory quantitative description of low-energy few-nucleon data, we propose here the simplest version of a new potential describing simultaneously (on the average) the main low-energy two-nucleon parameters and the binding energies of three and four nucleons. With this potential, we have found the three-nucleon binding energies and radii and compare the results with those for the M and AT potentials.

2. Statement of the Problem and Method of Research

Consider a nucleus ^{4}He in the ground state (the total spin $S = 0$) with the central exchange nuclear interaction potentials and with the Coulomb interaction between

the protons. The Hamiltonian of the four-nucleon system looks as

$$\hat{H} = -\frac{\hbar^2}{2m_p}(\Delta_1 + \Delta_2) - \frac{\hbar^2}{2m_n}(\Delta_3 + \Delta_4) +$$

$$+ \sum_{i>j=1}^{4} \hat{V}_{ij} + \frac{e^2}{|\mathbf{r}_1 - \mathbf{r}_2|}. \quad (1)$$

We study the problem in the center-of-mass frame. The pairwise nuclear potentials can be written in the form

$$\hat{V}_{ij} = [V_s^+(r_{ij})\hat{P}_s(\sigma) + V_t^+(r_{ij})\hat{P}_t(\sigma)](1 + \hat{P}_r)/2 +$$

$$+[V_s^-(r_{ij})\hat{P}_s(\sigma) + V_t^-(r_{ij})\hat{P}_t(\sigma)](1 - \hat{P}_r)/2\,, \quad (2)$$

where $\hat{P}_s$ and $\hat{P}_t$ are the projection operators onto the singlet and triplet spin states of two nucleons, and $\hat{P}_r$ is the Majorana operator of permutation of the spatial coordinates of particles. To study the system of four nucleons, we take advantage of the representation without isospin [4], treating protons and neutrons as different particles. The main advantage of the representation without isospin is the essential simplification of the system of equations for the spatial components of the wave function in comparison with the system of equations in the equivalent traditional isospin formalism (one has only two coupled equations instead of twelve ones). Therefore, to achieve a high controllable accuracy, it is more reasonable to use the representation without isospin. In this representation, the total wave function of a ^{4}He nucleus has the form

$$\Psi = \frac{1}{\sqrt{2}}(\xi'\Phi_1 - \xi''\Phi_2), \quad (3)$$

where Φ_1 and Φ_2 are the symmetric and antisymmetric spatial components, respectively, under the permutations of the identical protons $1 \rightleftarrows 2$ or identical neutrons $3 \rightleftarrows 4$, and ξ' and ξ'' are the corresponding spin functions for the total spin $S = 0$ and the Young scheme [2,2]. The total wave function is antisymmetric with respect to permutations of the protons or the neutrons. The system of equations for the spatial components Φ_1 and Φ_2 has the form [4]:

$$[\hat{K} + \frac{e^2}{r_{12}} + V^+_{s(pp)}(r_{12}) + V^+_{s(nn)}(r_{34}) +$$

$$+\frac{1}{8}\sum_{ij\neq 12,34}\sum_{+,-}(3V^{\pm}_{t(np)}(r_{ij}) + V^{\pm}_{s(np)}(r_{ij}))(1 \pm \hat{P}_r(ij)) -$$

$$-E]\Phi_1 + \frac{\sqrt{3}}{8}\sum_{ij\neq 12,34}\sum_{+,-}(-1)^{i+j}(V^{\pm}_{s(np)}(r_{ij}) -$$

$$-V^{\pm}_{t(np)}(r_{ij}))(1 \pm \hat{P}_r(ij))\Phi_2 = 0,$$

$$[\hat{K} + \frac{e^2}{r_{12}} + V^-_{t(pp)}(r_{12}) + V^-_{t(nn)}(r_{34}) +$$

$$+\frac{1}{8}\sum_{ij\neq 12,34}\sum_{+,-}(V^{\pm}_{t(np)}(r_{ij}) + 3V^{\pm}_{s(np)}(r_{ij}))(1 \pm \hat{P}_r(ij)) -$$

$$-E]\Phi_2 + \frac{\sqrt{3}}{8}\sum_{ij\neq 12,34}\sum_{+,-}(-1)^{i+j}(V^{\pm}_{s(np)}(r_{ij}) -$$

$$-V^{\pm}_{t(np)}(r_{ij}))(1 \pm \hat{P}_r(ij))\Phi_1 = 0. \quad (4)$$

Here, $\hat{K}$ is the kinetic energy operator, and $\hat{P}_r(ij)$ is the operator of permutation of the spatial coordinates of particles with numbers i and j. The subscripts (pp), (nn), and (np) at the potentials indicate the pairs of interacting nucleons (p means the proton, and n does the neutron). The system of equations (4) written in the representation without isospin can be also considered as a generalization of the equations for a ^{4}He nucleus onto the case where the interaction between nucleons is charge-dependent. In a short form, these equations look as

$$(\hat{H}_{11} - E)\Phi_1 + \hat{H}_{12}\Phi_2 = 0,$$

$$\hat{H}_{21}\Phi_1 + (\hat{H}_{22} - E)\Phi_2 = 0, \quad (5)$$

where $\hat{H}_{12} = \hat{H}_{21}$.

We study the bound state of ^{4}He on basis of Eqs. (4) using the variational Galerkin method with optimization of the Gaussian bases. This method has proved its high accuracy in the studies of few-particle systems with various interactions. Using the Gaussian basis, we will seek the spatial components of the variational function Φ_ν $(\nu = 1, 2)$ in the form

$$\Phi_\nu = \hat{S}_\nu \sum_{n=1}^{K_\nu} D_n^{(\nu)}\varphi_n^{(\nu)} \equiv$$

$$\equiv \hat{S}_\nu \sum_{n=1}^{K_\nu} D_n^{(\nu)} \exp(-\sum_{i>j=1}^{4} a_{ij}^{(\nu,n)} r_{ij}^2), \quad (6)$$

where φ_ν are the Gaussian basis functions, and K_ν is the dimension of the basis (K_1 for Φ_1, and K_2 for Φ_2). $\hat{S}_1$ is the symmetrization operator (for the function Φ_1), and $\hat{S}_2$ is the antisymmetrization operator (for the function

Φ_2) with respect to the permutations of identical particles (the protons $1 \rightleftarrows 2$ or the neutrons $3 \rightleftarrows 4$). The nonlinear parameters ${a_{ij}}^{(\nu,n)}$ are variational parameters. One of the advantages of the Gaussian representation of the wave function (6) is a simple explicit form of the matrix elements of operators in Eq. (4) to be of the same kind for all the basis elements. As known, the explicit form of the matrix elements can be derived directly. In particular, it is convenient to write the normalization in the form

$$\langle\varphi'|\varphi''\rangle = \pi^{\frac{9}{2}} U^{-\frac{3}{2}}, \tag{7}$$

where

$$U \equiv \sum_{i>j=1}^{4} \sum_{k>q=1}^{4} \sum_{\substack{m>l=1 \\ (ij)\neq(kq)\neq(ml)}}^{4} u_{ij}u_{kq}u_{ml},$$

$$u_{ij} \equiv a_{ij}^{\prime(\nu,n)} + a_{ij}^{\prime\prime(\nu,n)}. \tag{8}$$

The trilinear form U contains only the terms (their total quantity equals 16) that have compulsorily all four numbers of particles among the subscripts i, j, k, q, m, l. In expression (8), the primed nonlinear parameters appears from the left Gaussian function $\langle\varphi'|$, while the double-primed ones come from the right Gaussian function $|\varphi''\rangle$ in Eq. (7).

In this work, we consider the nuclear potentials in different states with radial dependence in the form of a superposition of the Gaussian functions $V(r_{ij}) = = \sum_k V_{(0)k} \exp(-b_k r_{ij}^2)$. In this case, the matrix elements of the potential energy $\langle\varphi'|V(r_{ij})|\varphi''\rangle$ look similar to expression (7), but with one of the terms u_{ij} changed by $\tilde{u}_{ij} = {a'_{ij}}^{(\nu,n)} + {a''_{ij}}^{(\nu,n)} + b_k$. Note that potential intensity parameters $V_{(0)k}$ and the parameters b_k determining the radii of the interaction potentials are, in general, different in different spin states and for the different kinds of nucleon pairs.

The matrix elements of the kinetic energy,

$$\langle\varphi'|\hat{K}|\varphi''\rangle \equiv -\sum_{i=1}^{4} \frac{\hbar^2}{2m_i}\langle\varphi'|\Delta_i|\varphi''\rangle, \tag{9}$$

can be written in the form (for the first particle)

$$-\frac{\hbar^2}{2m_1}\langle\varphi'|\Delta_1|\varphi''\rangle =$$

$$= \frac{\hbar^2}{2m_1}\frac{6\pi^{\frac{9}{2}}}{U^{\frac{5}{2}}}(a'_{12}a''_{12}(u_{13}u_{14}+u_{13}u_{24}+u_{13}u_{34}+$$

$$+u_{14}u_{23}+u_{14}u_{34}+u_{23}u_{24}+u_{23}u_{34}+u_{24}u_{34})+$$

$$+a'_{13}a''_{13}(u_{12}u_{14}+u_{12}u_{24}+u_{12}u_{34}+u_{14}u_{23}+$$

$$+u_{14}u_{24}+u_{23}u_{24}+u_{23}u_{34}+u_{24}u_{34})+$$

$$+a'_{14}a''_{14}(u_{12}u_{13}+u_{12}u_{23}+u_{12}u_{34}+u_{13}u_{23}+$$

$$+u_{13}u_{24}+u_{23}u_{24}+u_{23}u_{34}+u_{24}u_{34})+$$

$$+(a'_{12}a''_{13}+a'_{13}a''_{12})(u_{14}u_{23}+u_{23}u_{24}+u_{23}u_{34}+u_{24}u_{34})+$$

$$+(a'_{12}a''_{14}+a'_{14}a''_{12})(u_{13}u_{24}+u_{23}u_{24}+u_{23}u_{34}+u_{24}u_{34})+$$

$$+(a'_{13}a''_{14}+a'_{14}a''_{13})(u_{12}u_{34}+u_{23}u_{24}+u_{23}u_{34}+u_{24}u_{34})). \tag{10}$$

The expressions for three rest terms of the kinetic energy operator differ from (10) only by a permutation of the numbers of particles. The matrix element for the Coulomb interaction potential is also rather simple:

$$\langle\varphi'|\frac{e^2}{|\mathbf{r}_1-\mathbf{r}_2|}|\varphi''\rangle = \frac{2\pi^4 e^2}{U\sqrt{S}}. \tag{11}$$

Here,

$$S \equiv u_{13}u_{14}+u_{13}u_{24}+u_{13}u_{34}+u_{23}u_{14}+$$

$$+u_{23}u_{24}+u_{23}u_{34}+u_{14}u_{34}+u_{24}u_{34}\,. \tag{12}$$

The trilinear form U in (10) and (11) is defined by (8).

Within the Galerkin variational method, the bound states of a system can be found from the algebraic system of equations (which is actually the algebraic representation of the Schrödinger equation) determining the wave function linear expansion coefficients ${D_n}^{(\nu)}$:

$$\sum_{n=1}^{K_1} D_n^{(1)}(\langle S\varphi_j^{(1)}|\hat{H_{11}}|S\varphi_n^{(1)}\rangle - E\langle S\varphi_j^{(1)}|S\varphi_n^{(1)}\rangle)+$$

$$+\sum_{n=1}^{K_2} D_n^{(2)}\langle S\varphi_j^{(1)}|\hat{H_{12}}|S\varphi_n^{(2)}\rangle = 0,$$

$$\sum_{n=1}^{K_1} D_n^{(1)}\langle S\varphi_k^{(2)}|\hat{H_{21}}|S\varphi_n^{(1)}\rangle+$$

$$+\sum_{n=1}^{K_2} D_n^{(2)}(\langle S\varphi_k^{(2)}|\hat{H_{22}}|S\varphi_n^{(2)}\rangle - E\langle S\varphi_k^{(2)}|S\varphi_n^{(2)}\rangle) = 0,$$

$$j = 1, 2, ..., K_1;\ k = 1, 2, ..., K_2. \tag{13}$$

We recall that the linear coefficients ${D_n}^{(\nu)}$ are found within the Galerkin method from the system of linear

algebraic equations (13) for all the possible bound states. Within the Ritz method for the ground state energy (with the use of notations (5)), one has

$$E \le \frac{\langle\Psi|\hat{H}|\Psi\rangle}{\langle\Psi|\Psi\rangle} =$$

$$= \frac{\langle\Phi_1|\hat{H}_{11}|\Phi_1\rangle + 2\langle\Phi_1|\hat{H}_{12}|\Phi_2\rangle + \langle\Phi_2|\hat{H}_{22}|\Phi_2\rangle}{\langle\Phi_1|\Phi_1\rangle + \langle\Phi_2|\Phi_2\rangle}, \qquad (14)$$

and the above-mentioned coefficients become the variational parameters along with the rest ones (in particular, the nonlinear parameters $a_{ij}{}^{(\nu,n)}$ in the case of the Gaussian bases). As a result, to find the linear parameters within the Ritz method needs much greater efforts. But we used the Ritz method at some stages of precise calculations in the framework of the procedures of optimization (in the nonlinear parameters) of the Gaussian bases in order to speed up the calculations at the large dimensions of the bases. This is efficient due to the fact that, at small variations of a nonlinear parameter, the linear expansion coefficients in the double sums in the numerator and denominator of (14) can be considered approximately invariable (the double sums originate from the expansion of the wave function (6)). These sums are calculated rapidly, especially in the case of the variation of only one of the nonlinear parameters, when the main part of the terms of these sums remains fixed. On the other hand, within the Galerkin method, small variations of a nonlinear parameter make it necessary to solve the system of algebraic equations (13) once more. This may consume the essential time at large dimensions of the bases. Thus, it is efficient to use both methods in turn in order to have optimal calculational procedures.

To achieve a prescribed high accuracy in variational calculations at minimal dimensions of the Gaussian bases, it is essentially important to optimize the bases by varying the nonlinear parameters. We combine the stochastic methods of optimizing the Gaussian bases (see [1, 3])) efficient at the first stage of the optimization procedure with the regular methods [6–9] of optimization by varying several parameters or some groups of parameters. This enables us to obtain a high precision (the best in comparison with the results of other authors) in an optimal way and at moderate dimensions of the bases.

The bound states of three nucleons (the ^{3}He and ^{3}H nuclei) are also studied in the framework of the variational method with the use of Gaussian bases using the equations for spatial components of the wave function within the representation [4] without isospin. It is well known that the matrix elements of operators of the kinetic and potential energies of these systems have explicit simpler form than those for four nucleons. The procedure of optimal calculations of the bound states and all necessary three-particle values is very similar to that for four-particle values, by consuming the essentially less time due to a smaller number of variables and the simpler expressions for matrix elements to be computed. As to the two-nucleon problem, we use the standard methods of calculation of the deutron energy and its wave function. The two-particle phase shifts and the corresponding low-energy scattering parameters are found on the basis of the variable phase approach [10].

3. Binding Energies and Radii of Few-Nucleon Systems

The calculations of the binding energies and radii of few-nucleon nuclei are carried out for several semirealistic nuclear potentials. Table 1 contains the parameters of the used interaction potentials M and AT$^+$ (their components are denoted as $V^+{}_{s(nn)} = V^+{}_{s(pp)} = V^+{}_{s(np)} = V_s$, $V^+{}_{t(np)} = V_t$, all the odd parity components being equal zero). In addition, the properties of a ^{4}He nucleus are studied for the interaction potential AT having the components of odd parity equal to those

T a b l e 1. Parameters of potentials and the two-nucleon low-energy parameters (energies and intensities of potentials are given in MeV, scattering lengths and radii – in fm)

Potential	$V_t(r)$	$V_s(r)$	$B(D)$	a_t	a_s	r_{0t}	r_{0s}
M	$200\exp(-1.487r^2)-$ $-178\exp(-0.639r^2)$	$200\exp(-1.487r^2)-$ $-91.85\exp(-0.465r^2)$	2.202269	5.427	−16.804	1.758	2.885
AT	$1000\exp(-3r^2)-$ $-326.7\exp(-1.05r^2)-$ $-43\exp(-0.6r^2)$	$1000\exp(-3r^2)-$ $-166\exp(-0.8r^2)-$ $-23\exp(-0.4r^2)$	2.215822	5.391	−16.312	1.731	2.742
K1	$23789.46\exp(-(r/0.42)^2)-$ $-1169.92\exp(-(r/0.85)^2)$	$-27.38\exp(-(r/1.93)^2)$	2.224575	5.424	−23.748	1.79	2.932
	Experiment		2.224575	5.424	−23.748	1.75	2.75

of even parity, as well as for the potential AT* differing from AT by the absence of the triplet interaction between identical nucleons. All the above versions of potentials have sense and are used in the literature. In Table 1, we also present the parameters of the proposed new potential (to be denoted by K1). The main idea of constructing such a potential was to describe the main low-energy parameters of a two-nucleon system simultaneously with the energies of three- and four-nucleon systems. For the presented simplest version of the potential (containing a small number of parameters), the deuteron binding energy $B(D)$, the triplet a_t and singlet a_s scattering lengths were fitted exactly, and the binding energies of the nuclei ^{3}H, ^{3}He, and ^{4}He were fitted on average (the energies of ^{3}H and ^{3}He – with the accuracy of ~ 0.1 MeV, and the energy of ^{4}He – about ~ 0.3 MeV).

In the course of computations of the bound state of ^{4}He, it is established that the channel of the symmetric spatial wave function Φ_1 from (4) makes the decisive contribution to the system energy, whereas the role of the antisymmetric Φ_2 is less important. Thus, it has sense to achieve a closer approximation for, first of all, the symmetric spatial component of the wave function by using the expansion of basis functions. The optimal ratio is found for the corresponding dimensions K_1 and K_2 in the expansion (6) to be $K_1 \approx 3K_2$. Generally, the sufficient total dimension is to be within the range of two or three hundreds of basis functions in order to have the results for binding energies correct up to the third digit after the decimal point. By the way, for the case of potential M, the dimension of the basis should be noticeably less than that for potentials AT or K1, since the latter potentials have essentially more intense repulsion and more rapid change in their behavior in space. The intense short-range repulsion of a potential leads to an abrupt change in the behavior of the system's wave function, and we need a considerable amount of the Gaussian basis functions from (6) to properly reproduce it.

Using the obtained simple precise variational functions (6), we calculate the r.m.s. radii of the distribution of protons R_p and that of neutrons R_n, as well as the mass distribution radius R_m which obeys the relation ${R_m}^2 = \frac{1}{2}({R_p}^2 + {R_n}^2)$. As seen from Table 2, the radii R_p in a ^{4}He nucleus are somewhat greater than the corresponding radii R_n due to the Coulomb repulsion between the protons. It also follows from Table 2 that the proposed potential K1 gives better results both for the binding energy and radii of ^{4}He. To compare our results with those of other authors, we cite (in parentheses) some results of calculations by Varga and Suzuki [3] obtained by the stochastic method within the variational approach with the use of Gaussian bases and in the framework of the traditional isospin formalism.

Our results of variational calculations of the binding energy with the M potential ($B(^4\text{He}) = 29.948$ MeV) and the AT* potential ($B(^4\text{He}) = 30.376$ MeV) are the best in accuracy (only the last decimal digit can contain an error) and are obtained within a more efficient approach than the results from [3]. In Table 3, we give the binding energies and r.m.s. radii (R_p and R_n are, respectively, the radii of the distributions of protons and

T a b l e 2. Binding energy and r.m.s. radii of ^{4}He nucleus (in parenthesis, the results from [3] are cited)

Potential	M	AT$^+$	AT	AT*	K1	Experiment
$B(^4\text{He})$, MeV	29.948 (29.937)	29.733	30.827	30.376 (30.37)	28.60	28.296
$R_m(^4\text{He})$, fm	1.411 (1.41)	1.430	1.417	1.422 (1.42)	1.442	
$R_p(^4\text{He})$, fm	1.413	1.432	1.419	1.425	1.445	1.47
$R_n(^4\text{He})$, fm	1.408	1.428	1.414	1.420	1.439	

T a b l e 3. Binding energies and r.m.s. radii of the ^{3}H and ^{3}He nuclei

Potential	M	AT$^+$	AT	K1	Experiment
$B(^3\text{H})$, MeV	8,389	8,494	8.765	8.467	8.482
$R_m(^3\text{H})$, fm	1.706	1.693	1.673	1.708	
$R_p(^3\text{H})$, fm	1.586	1.576	1.546	1.602	1.57
$R_n(^3\text{H})$, fm	1.763	1.749	1.733	1.758	
$B(^3\text{He})$, MeV	7.712	7.836	8.110	7.758	7.718
$R_m(^3\text{He})$, fm	1.736	1.720	1.698	1.738	
$R_p(^3\text{He})$, fm	1.798	1.780	1.763	1.794	1.70
$R_n(^3\text{He})$, fm	1.604	1.593	1.560	1.621	
$E_C = B(^3\text{H}) - B(^3\text{He})$, MeV	0.677	0.658	0.655	0.709	0.764

neutrons, and R_m correponds to the mass distribution) also for ^{3}H and ^{3}He nuclei.

The r.m.s. radius of the mass distribution for a ^{3}H nucleus is defined as $R_m = (\frac{1}{3}R_p^2 + \frac{2}{3}R_n^2)^{\frac{1}{2}}$, and that for ^{3}He – as $R_m = (\frac{1}{3}R_n^2 + \frac{2}{3}R_p^2)^{\frac{1}{2}}$. The essential difference between the radii of the distributions of protons and neutrons ($R_p > R_n$ for ^{3}He and $R_p < R_n$ for ^{3}H, as for mirror nuclei) is mainly due to a noticeable difference between the nuclear forces in the triplet state (where the attraction is greater) and in the singlet state (with a weaker attraction), while the role of the Coulomb interaction is not important. The calculated Coulomb energy $E_C = B(^3\text{He}) - B(^3\text{He})$ appears to be, as usual, less than the experimental value, and we did not resolve this problem. Nevertheless, the proposed potential K1 results in a somewhat better value for the Coulomb energy. But the complete explanation of this value is a well-known problem and needs, probably, the consideration of the quark structure of nucleons.

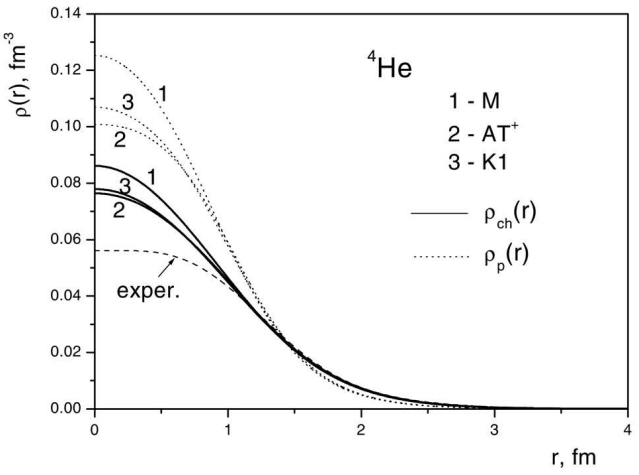

Fig. 1. Charge density distribution profiles of ^{4}He nucleus. Dotted curves show the profiles for the case of point-like nucleons, solid lines do the same for the case of non-point-like nucleons, and the dashed line depicts the experiment from [11]

4. Structure of a ^{4}He Nucleus

In the variational method with Gaussian bases, one obtains simultaneously the energy and the wave function of a system in a suitable Gaussian representation. This allows one, in particular, to analyze all the main structure functions of a ^{4}He nucleus. The density distribution of protons in a ^{4}He nucleus can be found (in the assumption of point-like nucleons) as

$$\rho_p(r) = \langle\Psi|\frac{1}{2}\sum_{k=1}^{2}\delta(\mathbf{r} - (\mathbf{r}_k - \mathbf{R}_{\text{c.m}}))|\Psi\rangle, \qquad (15)$$

where the wave function is normalized by unity. A similar expression can be written for the density distribution of neutrons $\rho_n(r)$ (changing the numbers of particles 1 and 2 by 3 and 4), and the mass density distribution of nucleons is $\rho_m(r) = \frac{1}{2}(\rho_p(r) + \rho_n(r))$. In Fig. 1, the dotted lines present the density distribution of protons in a ^{4}He nucleus for the potentials M (curve *1*), AT$^+$ (curve *2*), and K1 (curve *3*). Note that the density distribution of neutrons in a ^{4}He nucleus is almost the same as that of protons since the structure of the nucleus is determined by the nuclear forces (being charged-independent), and the Coulomb interaction is not essential. Due to the fact that the potentials AT$^+$ and K1 have more significant repulsion as compared with the M potential at short distances, the probability to find the nucleons at these distances for such potentials is substantially smaller. In spite of the fact that all the potentials have short-range repulsion, the density distributions do not manifest any "dips" at short distances for all the three cases of potentials. This is in concordance with the density distribution derived in [11] from the experimental charge formfactor obtained *ibidem* (with the model interpolation $F(q^2) \approx \approx (1 - (a^2q^2)^6)\exp(-b^2q^2)$, where the parameters $a = 0.316$ fm and $b = 0.681$ fm). The dashed line in Fig. 1 shows the charge density distribution which is the Fourier transform of this charge formfactor. To compare our results with this density distribution obtained from the experimental data for the formfactor, it is necessary, as usual, to take into account that nucleons are of finite size. Let $n_p(r)$ be the charge density distribution of a proton (with normalization $\int n_p(r)d\mathbf{r} = 1$), and let $n_n(r)$ be that for a neutron (with the normalization $\int n_p(r)d\mathbf{r} = 0$, since the neutron is neutral). In view of the finite size of nucleons, the charge density distribution in a ^{4}He nucleus has the form of a convolution product (see, for example, [12])

$$\rho_{\text{ch}}(r) = \int \rho_p(\mathbf{r}-\mathbf{r}')n_p(r')d\mathbf{r}' + \int \rho_n(\mathbf{r}-\mathbf{r}')n_n(r')d\mathbf{r}', \qquad (16)$$

where the normalization is chosen to be $\int \rho_{\text{ch}}(r)d\mathbf{r} = 1$. In Fig. 1, the solid lines depict the charge density distributions calculated with the use of (16). In this case, the charge density distributions of individual nucleons are given by the expressions

$$n_p(r) = \frac{3\sqrt{3}}{\pi a_p^3}\exp(-2\sqrt{3}\frac{r}{a_p}),$$

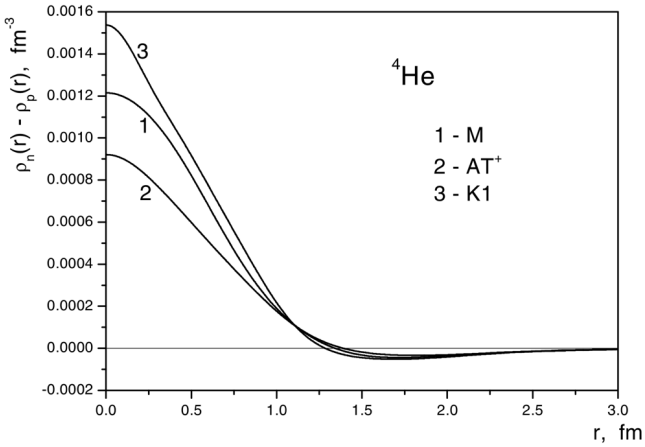

Fig. 2. Difference between the density distributions of neutrons and protons in a ^{4}He nucleus

$$n_n(r) = \frac{3\sqrt{3}}{\pi a_1^3}\exp(-2\sqrt{3}\frac{r}{a_1}) - \frac{3\sqrt{3}}{\pi a_2^3}\exp(-2\sqrt{3}\frac{r}{a_2}) \quad (17)$$

which follow from the simple interpolations of the experimental formfactors of nucleons [13, 14]

$$G_{E,p}(q^2) \approx (1 + \frac{1}{12}a_p^2 q^2)^{-2},$$

$$G_{E,n}(q^2) \approx (1 + \frac{1}{12}a_1^2 q^2)^{-2} - (1 + \frac{1}{12}a_2^2 q^2)^{-2} \quad (18)$$

with the parameters $a_p \approx 0.811$ fm, $a_1^2 \approx 0.58$ fm^2, $a_2^2 \approx 0.70$ fm^2. In our calculations, we used the latest value for the proton radius, $a_p \approx 0.875$ fm [15]. It follows from the analysis of the charge density distributions with the assumption that nucleons are not point-like particles that the results for the potentials AT$^+$ and K1 are closer to the experimental dotted line than that for the potential M, since the latter potential has weaker repulsion than the former ones. But, in all the cases, the calculated density at the nucleus center is noticeably greater than the experimental value. To achieve the complete accordance with the experiment, it is necessary to use potentials with even stronger repulsion and, perhaps, more adequate models of the nucleon structure.

To show the difference between the distributions of neutrons and protons (in the approximation of point-like nucleons) more clearly, we depict the difference $\rho_n(r) - \rho_p(r)$ in Fig. 2. Due to the Coulomb repulsion between protons, the density of neutrons at short distances in a ^{4}He nucleus is a little bit greater than the density of protons. At larger distances, the situation is inverse. This difference, relative to the density, is at most $\sim 1.5\%$. The neutron density excess at the nucleus center, being the most noticeable in the case of the K1 potential, is related to the fact that the neutrons in the singlet state can freely approach the short distances due to the absence of repulsion in the K1 potential in this state. On the contrary, the potential AT$^+$ has the strongest repulsion in the singlet state among the three considered ones, and, therefore, the neutron density excess is noticeably less. The M potential takes the intermediate position. The region of the proton density excess extends from ~ 1.4 fm to greater radii and becomes practically model-independent farther than a few fm, out of the range of nuclear forces.

Consider the formfactors of a ^{4}He nucleus. They are more sensitive to the short-range interaction between nucleons as compared with the density distributions. The formfactor of the distribution of protons is defined as

$$F_p(q^2) = \int \rho_p(r)\exp(-i(\mathbf{qr}))d\mathbf{r}. \quad (19)$$

A similar expression can be written for the formfactor of neutrons $F_n(q^2)$, and also for the mass distribution formfactor $F_m(q^2)$. To compare the calculated charge formfactor with the experiment, it is necessary to take into account that the nucleons are not point-like particles. Let $G_{E,p}(q^2)$ denote the charge formfactor of a single proton ($G_{E,p}(0) = 1$), and let $G_{E,n}(q^2)$ denote the same for a neutron ($G_{E,n}(0) = 0$, since the neutron is neutral). Then the charge formfactor of the ^{4}He nucleus is

$$F_E(q^2) = F_p(q^2)G_{E,p}(q^2) + F_n(q^2)G_{E,n}(q^2), \quad (20)$$

where $F_p(q^2)$ and $F_n(q^2)$ are found from the expressions of the type (19) containing the density distributions obtained for point-like nucleons. For the formfactors of lone nucleons we used parametrizations (18). The profiles of the absolute value of the charge formfactor (20) versus the momentum transfer squared are given in Fig. 3, both theoretical and experimental ones. All the curves contain a typical "dip" in the dependence on the momentum transfer squared at $q^2_{\min}$. We recall the experimental value $q^2_{\min,\exp} = 10.4$ fm^{-2} for the ^{4}He nucleus. The formfactor "dip" position is directly related to the amplitude of the scattering by the short-range repulsion between nucleons [16]. For an attractive potential without short-range repulsion, a "dip" in the formfactor is absent at all. For a potential with rather weak short-range repulsion, the "dip" takes place at comparatively large $q^2_{\min}$, whereas the repulsive core of a significant intensity results in the "dip" of the formfactor dependence at less $q^2_{\min}$, which is the known

fact and confirmed by the given examples as well. Note that the calculated formfactors for the AT$^+$ and K1 potentials are more close to the experiment than that for the M potential. We believe that the introduction of a short-range repulsion also into the K1 interaction in the singlet state will improve the concordance of the calculated formfactor with the experiment. Taking into account that nucleons are not point-like, i.e. more accurately treating the size of the nucleus, we make the behavior of the formfactor at small momenta transfer to be more close to the experimental one in comparison with that for the formfactor for point-like nucleons, because the behavior of the formfactor at small momenta transfer is uniquely bound with the r.m.s. radius of the nucleus, $\langle R^2\rangle^{\frac{1}{2}} = -6\frac{\partial}{\partial(q^2)}F(q^2)|_{q=0}$. At the same time, the formfactor decreases at large momenta transfer, if we take into account that the nucleons are not point-like, and the concordance with the experiment becomes worse within this range of momenta, which is the well-known problem. The position of the "dip" of the profile of the formfactor modulus is practically unchanged if one takes into account that nucleons are not point-like particles, because this "dip" is present due to the change of signs in the formfactors $F_p(q^2)$ and $F_n(q^2)$ for point-like nucleons.

Let us consider the pair correlation functions which reflect, in particular, the nucleon correlations at short distances. The proton-proton correlation function of the ^{4}He nucleus is defined as

$$g_{pp}(r) = \langle\Psi|\delta(\mathbf{r} - (\mathbf{r}_2 - \mathbf{r}_1))|\Psi\rangle. \quad (21)$$

A similar expression is valid for the neutron-neutron pair correlation function $g_{nn}(r)$ (substituting the numbers of particles 1 and 2 by 3 and 4). The neutron-proton pair correlation function is defined as follows:

$$g_{np}(r) = \langle\Psi|\frac{1}{4}\sum_{(ij)\neq(12),(34)}\delta(\mathbf{r} - (\mathbf{r}_i - \mathbf{r}_j))|\Psi\rangle. \quad (22)$$

Since the role of the Coulomb interaction in the ^{4}He nucleus is not essential, the functions $g_{pp}(r)$ and $g_{nn}(r)$ should be close to each other. But the neutron-proton pair correlation function $g_{np}(r)$ visibly differs from them, because the essentially more attractive triplet potential plays a more important role in the interaction between a neutron and a proton, than between the identical nucleons interacting in the singlet state, where a weaker singlet potential acts (assuming the charge-independent nuclear forces). Figure 4,*a* shows all three pair correlation functions in the case of the M potential, Fig. 4,*b* does the same for the AT$^+$ potential, and Fig. 4,*c* depicts the results for K1. It is seen in all the cases that, if a potential contains the short-range repulsion, it manifests itself directly in the behavior of the pair correlation functions at small distances in the form of a "dip". The decrease at small distances is absent only in $g_{pp}(r)$ and $g_{nn}(r)$ for the K1 potential, because our simplest model of interaction contains no repulsion in the singlet state. We hope that the introduction of a short-range repulsion into the improved versions of the potential should make the profiles of the pair correlation functions to be typical. It is important to emphasize that the pair correlation functions reflect, to a great extent, the behavior of the pairwise potentials, and they are very similar to the squared modulus of the two-particle wave function for the given potential. To confirm this fact, we give the squared modulus of the deuteron wave function $|\psi_D(r_{12})|^2 \equiv g_{np,D}(r_{12})$ in Fig. 4 by dashed lines (for respective potentials). They would almost coincide with the correlation functions $g_{np}(r)$ within the range of distances from zero to about 2 fm, if it were not the normalization factor (because of the contribution of large distances, where the deuteron wave function decreases slower due to the less binding energy of a deuteron). Only for the K1 potential, there exists a visible difference at short distances between the squared deuteron wave function (almost zero in the region of the strong core) and the pair correlation function $g_{np}(r)$, which is nonzero and has another behavior at short distances due to the contribution of the singlet channel present in the interaction between a neutron and a proton in a ^{4}He

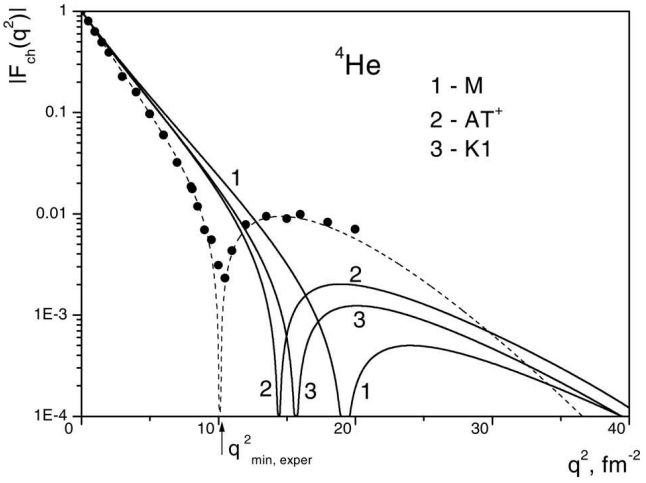

Fig. 3. Charge formfactor of a ^{4}He nucleus versus the momentum transfer squared. The dashed line depicts the interpolation of experimental data [11] (the dots correspond to the experimental values without error bars)

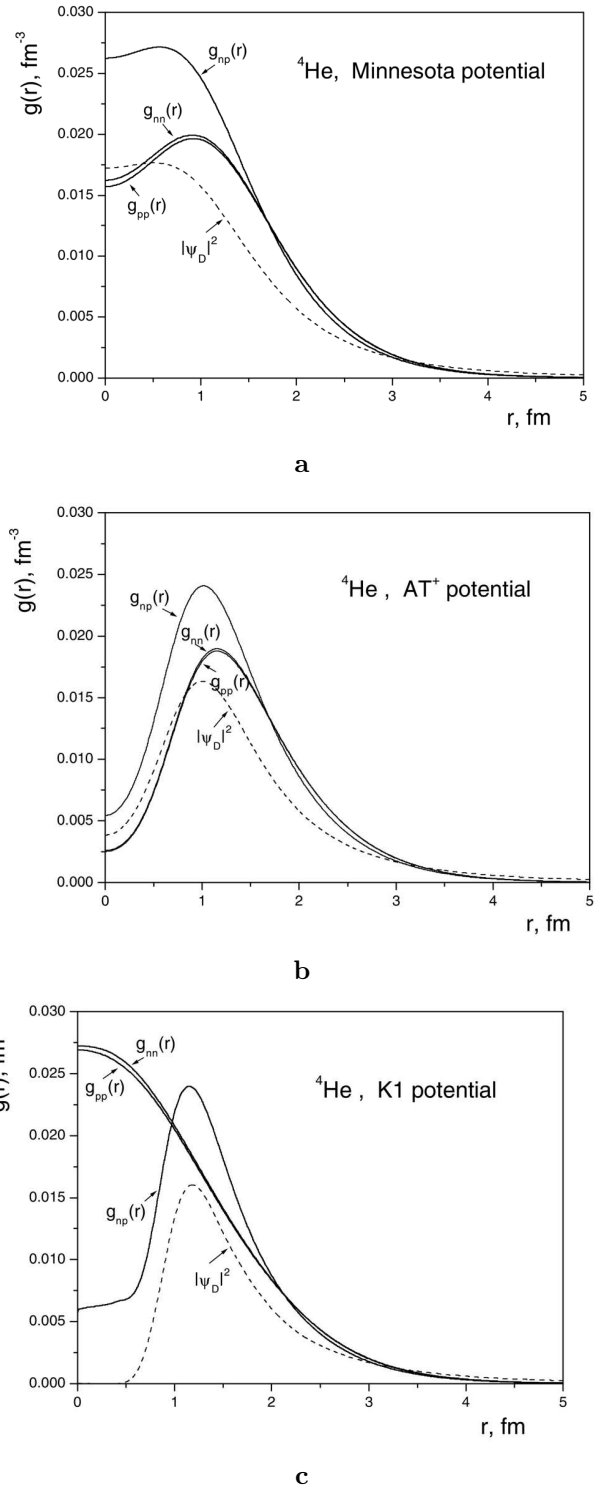

Fig. 4. The pair correlation functions of a ^{4}He nucleus for the potentials M (*a*), AT$^+$ (*b*), and K1 (*c*). The dashed line shows the squared deuteron wave function

nucleus (we recall that the singlet K1 interaction is purely attractive).

It is suitable to deal with the pair correlation functions separately for the singlet or triplet state. In particular, the neutron-proton pair correlation functions are defined as follows

$$g^{+}_{np,t}(r)=\frac{1}{4}\sum_{(ij)\neq(12),(34)}(\frac{3}{8}\langle\Phi_1|\delta(\mathbf{r}-\mathbf{r}_{ij})(1+\hat{P}_r(ij))|\Phi_1\rangle+$$

$$+\frac{1}{8}\langle\Phi_2|\delta(\mathbf{r}-\mathbf{r}_{ij})(1+\hat{P}_r(ij))|\Phi_2\rangle+$$

$$+\frac{\sqrt{3}}{4}\langle\Phi_1|(-1)^{i+j}\delta(\mathbf{r}-\mathbf{r}_{ij})(1+\hat{P}_r(ij))|\Phi_2\rangle),$$

$$g^{-}_{np,t}(r)=\frac{1}{4}\sum_{(ij)\neq(12),(34)}(\frac{3}{8}\langle\Phi_1|\delta(\mathbf{r}-\mathbf{r}_{ij})(1-\hat{P}_r(ij))|\Phi_1\rangle+$$

$$+\frac{1}{8}\langle\Phi_2|\delta(\mathbf{r}-\mathbf{r}_{ij})(1-\hat{P}_r(ij))|\Phi_2\rangle+$$

$$+\frac{\sqrt{3}}{4}\langle\Phi_1|(-1)^{i+j}\delta(\mathbf{r}-\mathbf{r}_{ij})(1-\hat{P}_r(ij))|\Phi_2\rangle),$$

$$g^{+}_{np,s}(r)=\frac{1}{4}\sum_{(ij)\neq(12),(34)}(\frac{1}{8}\langle\Phi_1|\delta(\mathbf{r}-\mathbf{r}_{ij})(1+\hat{P}_r(ij))|\Phi_1\rangle+$$

$$+\frac{3}{8}\langle\Phi_2|\delta(\mathbf{r}-\mathbf{r}_{ij})(1+\hat{P}_r(ij))|\Phi_2\rangle-$$

$$-\frac{\sqrt{3}}{4}\langle\Phi_1|(-1)^{i+j}\delta(\mathbf{r}-\mathbf{r}_{ij})(1+\hat{P}_r(ij))|\Phi_2\rangle),$$

$$g^{-}_{np,s}(r)=\frac{1}{4}\sum_{(ij)\neq(12),(34)}(\frac{1}{8}\langle\Phi_1|\delta(\mathbf{r}-\mathbf{r}_{ij})(1-\hat{P}_r(ij))|\Phi_1\rangle+$$

$$+\frac{3}{8}\langle\Phi_2|\delta(\mathbf{r}-\mathbf{r}_{ij})(1-\hat{P}_r(ij))|\Phi_2\rangle-$$

$$-\frac{\sqrt{3}}{4}\langle\Phi_1|(-1)^{i+j}\delta(\mathbf{r}-\mathbf{r}_{ij})(1-\hat{P}_r(ij))|\Phi_2\rangle). \qquad (23)$$

The sum over these functions results in (22) for $g_{np}(r)$, and only the total sum being normalized by unity. It is also interesting to consider the neutron-proton correlation functions for the triplet and singlet states, $g_{np,t} \equiv g^{+}_{np,t} + g^{-}_{np,t}$ and $g_{np,s} \equiv g^{+}_{np,s} + g^{-}_{np,s}$, respectively.

The singlet and triplet proton-proton pair correlation functions also can be formally subdivided into the functions for the states with even and odd parity,

$$g^{+}_{pp,s}(r) = \frac{1}{2}\langle\Phi_1|\delta(\mathbf{r}-\mathbf{r}_{12})(1+\hat{P}_r(12))|\Phi_1\rangle,$$

$$g^{-}_{pp,s}(r) = \frac{1}{2}\langle\Phi_1|\delta(\mathbf{r}-\mathbf{r}_{12})(1-\hat{P}_r(12))|\Phi_1\rangle,$$

$$g^{+}_{pp,t}(r) = \frac{1}{2}\langle\Phi_2|\delta(\mathbf{r}-\mathbf{r}_{12})(1+\hat{P}_r(12))|\Phi_2\rangle,$$

$$g^{-}_{pp,t}(r) = \frac{1}{2}\langle\Phi_2|\delta(\mathbf{r}-\mathbf{r}_{12})(1-\hat{P}_r(12))|\Phi_2\rangle, \qquad (24)$$

but it makes sense to consider simpler expressions for the pair correlation functions without such a subdivision by parity, the singlet correlation function $g_{pp,s} \equiv g^{+}_{pp,s} + g^{-}_{pp,s} = \langle\Phi_1|\delta(\mathbf{r}-\mathbf{r}_{12})|\Phi_1\rangle$ and the triplet one $g_{pp,t} \equiv g^{+}_{pp,t} + g^{-}_{pp,t} = \langle\Phi_2|\delta(\mathbf{r}-\mathbf{r}_{12})|\Phi_2\rangle$, since the protons interact in the definite states. The sum of functions (24) results in expression (21) for $g_{pp}(r)$ (and only the total function is normalized by unity). Expressions for the neutron-neutron correlation functions differ from (24) only by changing the numbers of particles (1 and 2 by 3 and 4), and their sum coincides with the expression for $g_{nn}(r)$. We emphasize that the analysis of the structure characteristics of pair correlation functions is important, because, in particular, the average potential energy of the system can be expressed in terms of these functions as

$$\langle\Psi|\hat{V}|\Psi\rangle = \sum_{\lambda}\int V_\lambda(r)g_\lambda(r)d\mathbf{r}, \qquad (25)$$

where the sum over λ means the summation over all the pairs of nucleons, over the triplet and singlet states, and over the parity states. In other words, each component of the nuclear interaction is integrated with a corresponding pair correlation function. Thus, the contribution of a potential into the energy depends not only on the interaction potential profile, but on the correlation function as well. Figure 5 depicts the pair correlation functions (23) for the potentials M and AT$^+$. It is evident that the triplet correlation functions exceed the singlet ones because the neutrons interact with the protons mainly in the triplet state (due to the statistical weight of this state, being three times greater, and because the triplet interaction between a neutron and a proton is more efficient in energy). Note that identical nucleons interact mainly in the singlet state. This is confirmed by small values of the triplet correlation functions of identical nucleons. In addition, the neutron-neutron correlation functions are close to the proton-proton ones (because of the insignificant role of the Coulomb interaction, as indicated above). It is interesting that, in the absence of the triplet interaction between identical nucleons, the triplet pair correlation function for these particles is, nevertheless, nonzero, though being small. This manifests some influence of the other nucleons of the nucleus on the given pair of nucleons, i.e. not everything in the many-particle system

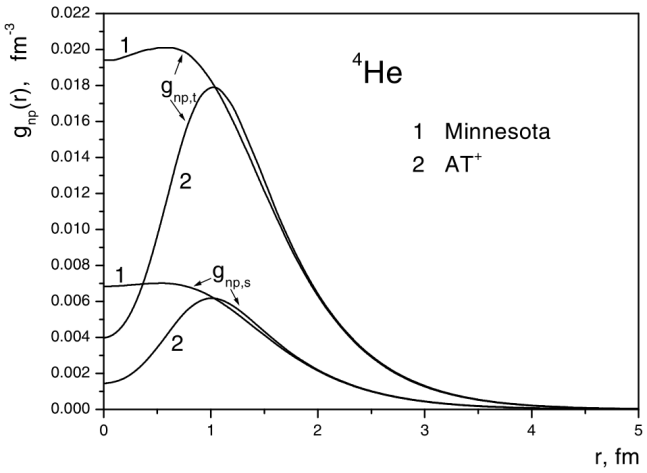

Fig. 5. Neutron-proton pair correlation functions of ^{4}He: $g_{np,t}(r)$ – for the triplet state, $g_{np,s}(r)$ – for the singlet state

with pairwise interactions can be reduced to the pair correlations only.

The averaged characteristics of the pair correlation functions are the correlation radii

$$r_{pp} = (\int r^2 g_{pp}(r)d\mathbf{r})^{\frac{1}{2}},$$

$$r_{nn} = (\int r^2 g_{nn}(r)d\mathbf{r})^{\frac{1}{2}},$$

$$r_{np} = (\int r^2 g_{np}(r)d\mathbf{r})^{\frac{1}{2}}, \qquad (26)$$

i.e. the root-mean-square distances between protons, neutrons, and between neutrons and protons, respectively (see Table 4). Using the distances between nucleons (26), one can find the radii (see Table 2)

$$R_p = \frac{1}{2}\sqrt{r^2_{np} + \frac{3}{4}r^2_{pp} - \frac{1}{4}r^2_{nn}},$$

$$R_n = \frac{1}{2}\sqrt{r^2_{np} + \frac{3}{4}r^2_{nn} - \frac{1}{4}r^2_{pp}},$$

$$R_m = \frac{1}{4}\sqrt{4r^2_{np} + r^2_{pp} + r^2_{nn}}, \qquad (27)$$

but we calculated all the values presented in the tables independently from one another.

T a b l e 4. Root-mean-square distances between the nucleons in the ^{4}He nucleus

Potential	M	AT$^+$	K1
r_{pp}, fm	2.368	2.401	2.403
r_{nn}, fm	2.357	2.391	2.385
r_{np}, fm	2.273	2.305	2.336

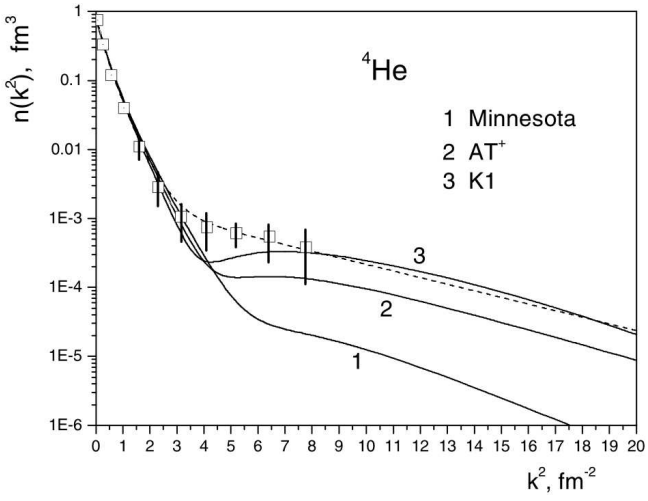

Fig. 6. Momentum distribution of protons in a ^{4}He nucleus. The experimental data (the squares with error bars) and the interpolation of the data (shown by the dashed line) are taken from [18]

Note that the distance between a neutron and a proton is shorter (due to the stronger attractive triplet interaction) than the distances between identical particles (interacting via the weaker attractive singlet interaction). As mentioned above, a small difference between r_{pp} and r_{nn} is related to a minor role of the Coulomb repulsion between protons (as a result, $r_{pp} > r_{nn}$).

The momentum distributions of protons, $n_p(k)$, and neutrons, $n_n(k)$, [17, 18] are the important structure functions of a ^{4}He nucleus. In terms of these functions, the average kinetic energy looks as

$$\langle \hat{K} \rangle = 2\Big(\int \frac{k^2}{2m_p} n_p(k) d\mathbf{k} + \int \frac{k^2}{2m_n} n_n(k) d\mathbf{k}\Big). \qquad (28)$$

By definition,

$$n_p(k) = \langle \tilde{\Psi} | \frac{1}{2} \sum_{i=1}^{2} \delta(\mathbf{k} - (\mathbf{k}_i - \mathbf{P}_{\mathrm{c.m}})) | \tilde{\Psi} \rangle, \qquad (29)$$

where the wave functions are in the momentum representation and are normalized by unity, and $\mathbf{P}_{\mathrm{c.m}}$ is the center-of-mass momentum. A similar definition is valid for $n_n(k)$ as well (with the sum over the third and fourth particles). Since the interaction between protons differs from that between neutrons by only the Coulomb potential slightly influencing (in comparison with the nuclear forces) the nucleus structure, the momentum distributions are to be almost identical both for neutrons and protons. Figure 6 shows the momentum distribution of protons for the potentials M, AT$^+$, and K1. The dashed line is the interpolation [18] of the experimental data for the proton momentum distribution in a ^{4}He nucleus. It is seen that, for low k^2, the momentum distributions are practically the same for all the potentials and coincide with the experimental data. This is explained by the correspondence between the small momenta and large distances of the system, i.e. the asymptotics of the wave function of a ^{4}He nucleus. Since the asymptotics of the wave function is practically model-independent and is determined by the binding energy of the nucleus (approximately the same for all the potentials), the momentum distributions at low momenta have almost the model-independent behavior. On the other hand, at higher k^2 because of the essential difference in the behaviors of potentials at short distances (i.e. due to the repulsion of different intensities), the momentum distributions reveal noticeably different dependences. The best concordance with the experiment (on the average) is appeared to be for the proposed potential K1. Note that the nucleon momentum distributions evidently show two regimes in their dependences on the momentum, which reflects the averaged behavior of potentials (low momenta) and the short-range repulsion (high momenta). Between the two regimes, there exists a certain "dip" in theoretical curves. One should keep in mind that the main contribution to the kinetic energy that can be expressed through the momentum distributions is made by just comparatively high momenta $k^2 \sim 10$ fm^{-2} due to the additional multiplier $\sim k^4$. Some of the known potentials (e.g., the M potential) appear to be absolutely inadequate for the description of this part of the momentum distribution. This potential has insufficiently rapid variation at short distances, in particular a deficient repulsion, in order to be able to reproduce the momentum distribution at $k^2 \sim 10$ fm^{-2}.

5. Summary

To summarize, we notice the main results. In this work, the ground state of the ^{4}He nucleus is studied with high controllable precision within the variational method, applying the optimization of the Gaussian bases and using the efficient representation without isospin. The energy and the main structure characteristics of this four-nucleon nucleus are studied for a few nuclear interaction potentials. We have obtained the best results for the binding energy and radii in comparison with those available for the commonly used Minnesota and Afnan-Tang potentials. The correspondence between the

structure functions of the nucleus and the pair interaction potentials behavior, in particular at short distances, is found. Starting from the idea to construct the nuclear potential for the simultaneous description of the few-nucleon data at low energies, we propose a simple preliminary version of a new NN-interaction potential which qualitatively correctly describes both the main low-energy parameters of two nucleons and the energies of three- and four-nucleon systems. It is found that the main structure functions of the four-nucleon system are also more satisfactorily described by this potential. We expect that the further efforts in this direction would enable to have more accurate simultaneous description of the main low-energy parameters of the few-nucleon systems and believe that such a potential might be used to treat more complicated nuclei.

With a profound gratitude, the authors think of the collaboration with A.I.Steshenko on the initial stage of this work.

1. V.I. Kukulin and V.M. Krasnopol'sky, J. Phys. G: Nucl.Phys. **3**, 795 (1977).
2. N.N. Kolesnikov and V.I. Tarasov, Yad. Fiz. **35**, 609 (1982).
3. K. Varga and Y. Suzuki, Phys. Rev. C **52**, 2885 (1995).
4. I.V. Simenog, I.S. Dotsenko, and B.E. Grinyuk, Ukr. Fiz. Zh. **47**, 129 (2002).
5. I.S. Dotsenko and I.V. Simenog, Ukr. Fiz. Zh. **51**, 841 (2006).
6. B.E. Grinyuk and I.V. Simenog, Ukr. Fiz. Zh. **45**, 21 (2000).
7. B.E. Grinyuk and I.V. Simenog, Ukr. Fiz. Zh. **45**, 625 (2000).
8. S.M. Bubin and I.V. Simenog, J. of Phys. Stud. **4**, 124 (2000).
9. B.E. Grinyuk, M.V. Kuzmenko, and I.V. Simenog, Ukr. Fiz. Zh. **48**, 1014 (2003).
10. V.V. Babikov, *The Variable Phase Approach in Quantum Mechanics* (Nauka, Moscow, 1976), 288 c. (in Russian)
11. R.F. Frosch, J.S. McCarthy, R.E. Rand, and M.R. Yearian, Phys. Rev. **160**, 874 (1967).
12. A.I. Akhiezer, A.G. Sitenko, and V.K. Tartakovsky, *Nuclear Electrodynamics* (Springer, Berlin, 1994).
13. W. Bertozzi, J. Friar, J. Heisenberg, and J.W. Negele, Phys. Lett. **41B**, 408 (1972).
14. P.E. Bosted et al., Phys. Rev. Lett. **68**, 3841 (1992).
15. *Nuclear and Particle Physics. Review of Particle Physics.* J. of Phys. G. **33**, 1 (2006).
16. B.E Grinyuk and I.V. Simenog, *Physics of Many-Particle Systems* (Naukova Dumka, Kyiv, 1985), pp. 66–95. (In Russian).
17. A.N. Antonov, P.E. Hodgson, and I.Zh. Petkov, *Nucleon Momentum and Density Distributions in Nuclei* (Clarendon Press, Oxford, 1988).
18. C. Ciofi degli Atti, S. Simula, Phys. Rev. C **54**, 1689 (1996).

Received 11.10.06

СТРУКТУРНІ ОСОБЛИВОСТІ ЯДРА ^{4}He
У МІКРОСКОПІЧНОМУ ПІДХОДІ

Б.Є. Гринюк, Д.В. П'ятницький, І.В. Сименог

Р е з ю м е

З високою точністю досліджено енергії, розміри і основні структурні функції ядра ^{4}He в рамках варіаційного методу з оптимізованими гаусоїдними базисами для потенціалів Міннесота, Афнана–Танга і запропонованого нового варіанта NN-потенціалу K1, який узгоджує основні низькоенергетичні параметри двох нуклонів і енергії три- та чотиринуклонних ядер. Проведено аналіз структурних особливостей ядра ^{4}He. Для досягнення прецизійної точності розрахунків малонуклонних систем використано переваги представлення без ізоспіну.